

Experimental Investigation of Combustion of Jet Fuels and Surrogates in Nonpremixed Flows

Stefan Humer,* Reinhard Seiser,† and Kalyanasundaram Seshadri‡
University of California, San Diego, La Jolla, California 92093

DOI: 10.2514/1.46916

Experimental studies are carried out to characterize nonpremixed combustion of jet fuels and a number of their surrogates in laminar nonuniform flows. The counterflow configuration is employed. Critical conditions of extinction and autoignition are measured for jet propellant 8, Jet-A, and Fisher–Tropsch jet propellant 8. Thirteen surrogates of jet propellant 8 and one surrogate of Fisher–Tropsch jet propellant 8 are tested. It is found that critical conditions of extinction and autoignition of jet propellant 8 and Jet-A are similar, while Fisher–Tropsch jet propellant 8 is more reactive than jet propellant 8 and Jet-A. Among the surrogates tested, surrogate H [made up of *n*-decane (80%) and 1, 3, 5-trimethylbenzene (20%) by liquid volume] and surrogate C [made up of *n*-dodecane (60%), methylcyclohexane (20%), and *o*-xylene (20%) by liquid volume] best reproduce extinction and autoignition characteristics of jet propellant 8. Surrogate G [made up of *n*-decane (60%) and iso-octane (40%) by liquid volume] best reproduces the combustion characteristics of Fisher–Tropsch jet propellant 8.

I. Introduction

CHARACTERIZING the combustion of commercial fuels is of practical importance. The focus of the present work is on jet fuels: Jet-A, jet propellant 8 (JP-8), and Fisher–Tropsch (FT) JP-8. Jet-A is used in commercial aviation, while JP-8 is used by the U.S. Air Force. The U.S. Army is developing technologies for converting diesel-powered equipment so that they can be powered by JP-8. Jet fuels are a mixture of numerous aliphatic and aromatic compounds. The major components of this fuel are straight-chain paraffins, branched-chain paraffins, cycloparaffins, aromatics, and alkenes [1–6]. The concentration of paraffins is, on the average, 60% by volume; that of cycloparaffins is 20%, that of aromatics is 18%, and that of alkenes is 2%. It has been established that a useful approach to understanding combustion of jet fuels is to first develop surrogates that reproduce selected aspects of combustion of these types of fuels. Surrogates are mixtures of hydrocarbon compounds. The components in the surrogate will depend on those aspects of combustion of jet fuels that the surrogate is expected to reproduce. The present work is devoted to characterizing aspects of combustion of jet fuels and their surrogates in nonuniform, laminar flows at atmospheric pressure.

Reports from several workshops have outlined the procedures to be employed to develop surrogates for JP-8, diesel, and gasoline [1]. It has been suggested that the components in the surrogate will depend on the application or targets. The working group for jet fuel surrogates has recommended a list of components that could be used to develop surrogates. The list includes straight-chain alkanes (*n*-decane, *n*-dodecane, and *n*-tetradecane), branched-chain alkanes (iso-octane and isocetane), cycloalkanes (ethyl/propyl/butylcyclohexanes and decalin), single-ring aromatics (ethyl/propyl/butylbenzenes), and multiring aromatics (1-methylnaphthalene). In addition to these compounds, methylcyclohexane, toluene, *o*-xylene, and

trimethylbenzene are included in the list of components to be tested here, because some of these compounds have been employed successfully in a previous study on surrogates for JP-8 [7].

Starting from the pioneering work of Schulz [8], who proposed a 12-component surrogate mixture for JP-8, several investigators have proposed surrogates for jet fuels [2–7,9–18]. Dean et al. [12] studied autoignition of Jet-A and mixtures of benzene, hexane, and decane in air using a heated shock tube at mean shock pressures of 8.5 ± 1 atm within a temperature range of 1000–1700 K. Ignition delay times in 20% hexane/80% *n*-decane, 20% benzene/80% *n*-decane, and 18.2% benzene/9.1% hexane/72.7% *n*-decane mixtures at a temperature range between 1450–1750 K correlate well with ignition delay times for Jet-A. Thus, these mixtures can be considered as possible surrogates for aviation kerosene [12]. Agosta et al. [2] have suggested possible components of a surrogate that reproduces reaction behavior of jet fuels. The components *n*-dodecane and isocetane are the reference components for alkanes; methylcyclohexane and decalin represent cyclohexanes, and 1-methylnaphthalene represents aromatics [2]. Guéret et al. [13] studied oxidation of kerosene fuel and oxidation of a mixture of 79% undecane, 10% propylcyclohexane, and 11% trimethylbenzene in a jet-stirred flow reactor in the temperature range of 873–1033 K at atmospheric pressure. The reaction products formed during the oxidation of kerosene and the ternary mixture were similar [13]. Quasi-global chemical-kinetic models were developed to reproduce experimental data. Dagaut et al. [14] modeled kerosene combustion in a jet-stirred reactor using *n*-decane. Lindstedt and Maurice [15] calculated the structure of premixed *n*-decane flames and compared their results with experimental data. Experimental data show that there exists similarities between the structure of *n*-decane flames and kerosene flames. Lindstedt and Maurice [15] modeled the structure of kerosene flames using a surrogate blend comprising 89 mol% *n*-decane and 11 mol% aromatic fuel. The aromatic component was represented by 1) benzene, 2) toluene, 3) ethylbenzene, and 4) ethylbenzene/naphthalene [15]. The calculated structure was compared with experimental data. Patterson et al. [16] assumed a mixture of 89% *n*-decane and 11% toluene as a surrogate for kerosene. They computed the structure of counterflow diffusion flames using this surrogate. Edwards and Maurice [3] reported that a mixture of iso-octane, methyl cyclohexane, *m*-xylene, cyclo-octane, decane, butylbenzene, 1,2,4,5-tetramethylbenzene, tetraline, dodecane, 1-methylnaphthalene, tetradecane, and hexadecane is a possible surrogate for JP-8. Montgomery et al [17] presumed that a mixture of 34.7% *n*-dodecane, 32.6% *n*-decane, 16.0% butylbenzene, and 16.7% methylcyclohexane is a surrogate for JP-8. They developed a reduced chemical-kinetic mechanism for the surrogate using the

Received 29 August 2009; revision received 19 August 2010; accepted for publication 11 January 2011. Copyright © 2011 by the American Institute of Aeronautics and Astronautics, Inc. All rights reserved. Copies of this paper may be made for personal or internal use, on condition that the copier pay the \$10.00 per-copy fee to the Copyright Clearance Center, Inc., 222 Rosewood Drive, Danvers, MA 01923; include the code 0748-4658/11 and \$10.00 in correspondence with the CCC.

*Postdoctoral Research Associate, Department of Mechanical and Aerospace Engineering.

†Research Scientist, Department of Mechanical and Aerospace Engineering.

‡Professor of Fluid Mechanics, Department of Mechanical and Aerospace Engineering.

computer-assisted reduction method [17,18]. The reduced mechanism was tested by comparing profiles of temperature and concentration of various species obtained using this mechanism with those calculated using a detailed mechanism. Violi et al. [5] modeled kerosene fuel by a surrogate blend composed of 73.5 mol% *n*-dodecane, 5.5 mol% *i*-octane, 10 mol% methylcyclohexane, and 11 mol% of aromatic fuel components. The aromatic component was represented computationally by 9 mol% benzene and 91 mol% toluene [5]. Edwards [4] has shown results of compositional analysis of kerosene fuels. The analysis suggests that a surrogate model for JP-8 should be made up of 18% aromatics: the aromatics should be a C_{10} alkylbenzene, and the nonaromatic component should be an isoparaffin and/or naphthene. The choice of the fuels to be tested here is motivated by these previous studies.

Previous experimental studies on liquid hydrocarbon fuels were focused on measuring ignition delay times in shock tubes [12,19–21] and rapid compression machines [22–25]. Studies on liquid fuels in jet-stirred flow reactors [13,26,27] and premixed flames stabilized on flat flame burners are available [28]. These experimental studies were conducted on premixed systems in the absence of fluid flow. Studies on counterflow nonpremixed flames [9,29–32] and premixed flames [33] are also available. Honnet et al. [9] carried out experimental and numerical studies to develop a surrogate that can reproduce selected aspects of combustion of kerosene. A mixture of *n*-decane 82% and 1, 2, 4-trimethylbenzene 18% by volume (*n*-decane 80% and 1, 2, 4-trimethylbenzene 20% by weight) called the Aachen surrogate was tested. Critical conditions of extinction, autoignition, and volume fraction of soot measured in laminar nonpremixed flows burning the Aachen surrogate were found to be similar to those in flames burning kerosene [9].

Here, an experimental investigation is carried out with the aim of developing an appropriate surrogate for jet fuels and FT JP-8. The counterflow configuration is employed. Critical conditions of extinction and autoignition are measured for various jet fuels in nonpremixed systems. Similar measurements are made for potential surrogates of these fuels. The results of the present work are particularly useful for developing technologies for converting diesel-powered equipment so that they can be powered by JP-8. For this reason, the studies are performed on nonpremixed systems. The conversion is a complicated process. Many issues with fuel properties and performance have to be considered. They include autoignition, combustion, fuel injection, lubricity, and spray characteristics. Autoignition is considered here because it plays a key role in performance of compression-ignition engines.

II. Experimental Apparatus and Procedures

Figure 1 is a schematic illustration of the experimental setup. It shows the counterflow flowfield; the air, nitrogen, and fuel feed systems; and the vaporizer.

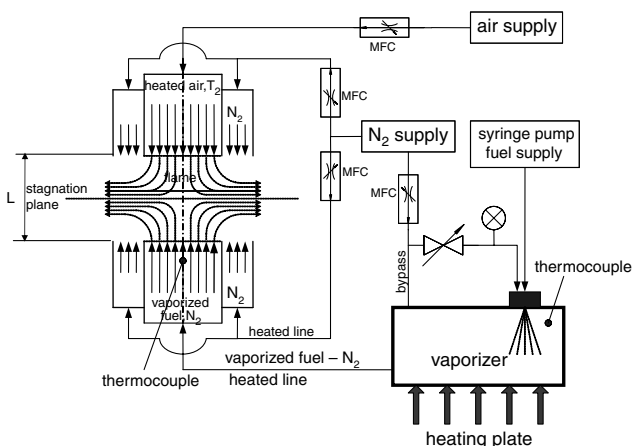


Fig. 1 Schematic illustration of experimental setup. Figure shows counterflow flowfield; air, nitrogen, and fuel feed systems; and vaporizer.

by injecting them into a heated chamber by an air blast nozzle. The temperature is kept about 20 K above the boiling range to assure that all its components are vaporized. Two thermocouples are used to monitor the temperature inside the vaporizer. One is placed close to the nozzle, and the other is placed at the exit of the vaporizer chamber. Flow rates of gases are adjusted by computer-regulated mass flow controllers. Flow lines going from the vaporizer to the counterflow burner are heated to prevent condensation inside the lines. A detailed description of the burner is given elsewhere [29,30]. The boiling points for all the fuels tested here are less than 600 K. At these temperatures, very little breakdown of the fuel takes place. Gas-chromatograph/mass-spectrometer (GC/MS) analysis of the vapors of JP-8 was carried out before the fuel was introduced into the vaporizer and after it was injected from the exit of the fuel duct. Comparison of the results shows that there is very little breakdown of the fuel in the vaporizer. Details of the analysis are given in the Appendix.

In the burner, a fuel stream made up of prevaporized fuel and nitrogen is injected from the fuel duct, and an oxidizer stream of air is injected from the oxidizer duct. These jets flow into the mixing layer between the two ducts. The exit of the fuel duct is called the fuel boundary, and the exit of the oxidizer duct is called the oxidizer boundary. The mass fraction of the fuel, the temperature, and the component of the flow velocity normal to the stagnation plane at the fuel boundary are represented by $Y_{F,1}$, T_1 , and V_1 , respectively. The mass fraction of the oxygen, the temperature, and the component of the flow velocity normal to the stagnation plane at the oxidizer boundary are represented by $Y_{O_2,2}$, T_2 , and V_2 , respectively. The distance between the fuel boundary and the oxidizer boundary is represented by L . The velocities of the reactants at the boundaries of the counterflow burner are presumed to be equal to the ratio of their volumetric flow rates to the cross-sectional area of the ducts. The temperature of the fuel stream and the temperature of the oxidizer stream at the boundaries are measured using a bare Pt–Pt13%Rh (type R) thermocouple. The wire diameter is 0.076 mm and the bead diameter is 0.21 mm. The leads of the thermocouple are aligned along the isotherms in the radial direction to minimize conductive heat losses. Close to the exits of the ducts, the axial gradients of temperature are also expected to be small. The measurement is corrected for radiation by employing the formulation $Nu(T_g - T_i)\lambda/d = \epsilon T_i^4$. Here, T_g is the gas temperature, T_i is the temperature recorded by the thermocouple, d is the diameter of the bead, λ is the thermal conductivity of the gas, the Nusselt number is $Nu = 2$, and the emissivity is $\epsilon = 0.128$. The leads of the thermocouple are aligned along the isotherms in the radial direction to minimize conductive heat losses.

The value of the strain rate, defined as the normal gradient of the normal component of the flow velocity, changes from the fuel boundary to the oxidizer boundary [34]. The characteristic strain rate on the oxidizer side of the stagnation plane a_2 is presumed to be given by [34]

$$a_2 = \frac{2|V_2|}{L} \left(1 + \frac{|V_1|\sqrt{\rho_1}}{|V_2|\sqrt{\rho_2}} \right) \quad (1)$$

Here, ρ_1 and ρ_2 represent the density of the mixture at the fuel boundary and at the oxidizer boundary, respectively. The momentum of the counterflowing streams are approximately maintained at the same value to ensure that the stagnation plane is at midplane between the two ducts. Equation (1) is obtained from an asymptotic theory where the Reynolds numbers of the laminar flow at the boundaries are presumed to be large [34]. Critical conditions of extinction are presumed to be given by the strain rate $a_{2,e}$ and the mass fraction of fuel at the fuel boundary. Critical conditions of autoignition are presumed to be given by the strain rate $a_{2,i}$, the temperature of the oxidizer stream $T_{2,i}$, and the mass fraction of fuel at the fuel boundary.

The fuels tested include 1) jet fuels, 2) surrogates of JP-8, and 3) a surrogate of FT JP-8. The molar ratio of hydrogen to carbon in these fuels is represented by H/C. Different batches of jet fuels tested here

Table 1 Components of Jet-A, JP-8, and FT JP-8^a

	Summarized D 2425, vol%					
	3602 Jet-A	3638 Jet-A	4177 JP-8	3773 JP-8	4658 Jet-A blend	4734 FT JP-8
Paraffins	49.4	64.5	51.3	61.6	48	>99
Cycloparaffins	15.8	13.2	18	15.5	26	<1
Dicycloparaffins	10.8	7.1	11.8	5.7	6	<1
Tricycloparaffins	0.9	0.6	1.6	0.5	<1	<1
Alkylbenzenes	14	10.8	9.3	12	13	<0.5
Indan and tetralins	7.9	2.1	6.7	3.1	4.6	<0.5
Indenes $C_nH_{(2n-10)}$	<0.2	<0.2	<0.2	<0.2	<0.5	<0.5
Naphthalene	<0.2	0.4	<0.2	<0.2	<0.5	<0.5
Naphthalenes	1.2	1.3	1	1.5	1.4	<0.5
Acenaphthenes	<0.2	<0.2	0.2	<0.2	<0.5	<0.5
Acenaphthylenes	<0.2	<0.2	<0.2	<0.2	<0.5	<0.5
Tricyclic aromatics	<0.2	<0.2	<0.2	<0.2	<0.5	<0.5
Total	100	100	100	100	100	100

^aT. James Edwards, private communication, 2010.

are identified by a number following POSF, which is an in-house notation used by the U.S. Air Force Research Laboratory for identifying various fuels.

1) The types of jet fuels tested are described next:

a) The different batches of jet propellant 8 tested are JP-8 (obtained from Naval Air Warfare Center, China Lake, California), JP-8 POSF 4177 [obtained from Wright-Patterson Air Force Base (WPAFB)], and JP-8 POSF 3773 (obtained from WPAFB). The average chemical formula is $C_{12}H_{23.3}$, $H/C = 1.91$. Components are shown in Table 1.

b) The different batches of commercial aviation fuels tested are Jet-A (obtained from San Diego Airport), Jet-A POSF 3602 (obtained from WPAFB), Jet-A POSF 3638 (obtained from WPAFB), and blend POSF 4658 (obtained from WPAFB). The average chemical formula is $C_{12}H_{23.3}$, $H/C = 1.91$. Components are shown in Table 1.

c) A FT JP-8 was also tested (obtained from WPAFB). Components are shown in Table 1.

2) Surrogates of JP-8 are fuel mixtures (liquid volume). The surrogates tested are a) surrogate A: 60% *n*-decane, 20% methylcyclohexane, 20% toluene ($H/C = 1.93$); b) surrogate B: 60% *n*-decane, 20% methylcyclohexane, 20% *o*-xylene ($H/C = 1.93$); c) surrogate C: 60% *n*-dodecane, 20% methylcyclohexane, 20% *o*-xylene ($H/C = 1.92$); d) surrogate D: *n*-decane 50%, butylcyclohexane 25%, butylbenzene 25% ($H/C = 1.92$); e) surrogate E: *n*-decane 34%, butylcyclohexane 33%, butylbenzene 33% ($H/C = 1.84$); f) surrogate F: *n*-decane 60%, butylcyclohexane 20%, butylbenzene 20% ($H/C = 1.97$); g) surrogate H: *n*-decane 80%, 1,3,5-trimethylbenzene 20% ($H/C = 1.99$); h) surrogate J: *n*-dodecane 80%, 1,3,5-trimethylbenzene 20% ($H/C = 1.97$); i) surrogate NI: *n*-decane 80%, propylbenzene 20%; j) surrogate N2: *n*-decane 70%, propylbenzene 30%; k) Drexel surrogate 1: *n*-dodecane 26%, isocetane 36%, methylcyclohexane 14%, decaline 6%, and 1-methylnaphthalene 18% ($H/C = 1.82$); 12) Drexel surrogate 2: *n*-dodecane 43%, isocetane 27%, methylcyclohexane 15%, and 1-methylnaphthalene 15% ($H/C = 1.87$); and 13) Utah surrogate: *n*-dodecane 30%, *n*-tetradecane 20%, iso-octane 10%, methylcyclohexane 20%, *o*-xylene 15%, and tetraline 5% ($H/C = 1.93$).

3) A possible surrogate of FT JP-8 tested is a) surrogate G: *n*-decane 60%, iso-octane 40% ($H/C = 2.22$).

Surrogate A, surrogate B, and surrogate C have been tested previously [7]. They are included here for comparison with other surrogates. Surrogate D has been suggested as a possible surrogate of diesel. It is tested here to check if it could also be used as a surrogate for jet fuels. Surrogate E and surrogate F have the same components as surrogate D, with different concentrations. The components in surrogate H are the same as those suggested previously for surrogates of kerosene [35]. In surrogate J, the *n*-decane in surrogate H is replaced by *n*-dodecane. In surrogate NI and surrogate N2, 1,3,5-trimethylbenzene in surrogate H is replaced by propylbenzene. The

Drexel surrogate 1 was tested in [2]. The Drexel surrogate 2 is a modification of Drexel surrogate 1. The Utah surrogate is the same as that tested in [5], with *m*-xylene in [5] replaced by *o*-xylene.

Critical conditions of extinction and autoignition are measured. They depend on six parameters. They are the pressure p and the quantities a_2 , $Y_{F,1}$, T_1 , $Y_{O_2,2}$, and T_2 . The experiments are carried out at atmospheric pressure. The oxidizer stream is air with $Y_{O_2,2} = 0.233$. The temperature of the fuel stream is $T_1 = 473(\pm 10)$ K. This fixes three of the six parameters. The extinction experiments are carried out with $T_2 = 298$ K. At some selected value of $Y_{F,1}$, the flame is stabilized at $a_2 < a_{2,e}$. The strain rate is increased by increasing V_1 and V_2 until extinction is observed. The strain rate at extinction $a_{2,e}$ is recorded as a function of mass fraction of $Y_{F,1}$. The accuracy of the strain rate is $\pm 10\%$ of the recorded value, and that of the fuel mass fraction is $\pm 3\%$ of the recorded value. The experimental repeatability on the reported strain rate is $\pm 5\%$ of the recorded value, and that of the fuel mass fraction is $\pm 1\%$ of the recorded value. The experimental results are shown later.

Two sets of experiments are carried out to establish the critical conditions of autoignition. In one set, $Y_{F,1} = 0.4$. At chosen values of strain rate, the flowfield is established. The temperature of air is increased until autoignition takes place. The onset of autoignition is observed using a high-speed camera to make sure that ignition takes place close to the axis of symmetry. The temperature of the air stream $T_{2,i}$ is recorded as a function of the strain rate $a_{2,i}$. The accuracy of the measurement of the temperature of air at autoignition is expected to be ± 30 K, the strain rate is expected to be $\pm 10\%$, and the fuel mass fraction is expected to be $\pm 3\%$ of the recorded value. The experimental repeatability in the measurement of the temperature of air at autoignition is expected to be ± 6 K, that of strain rate is expected to be $\pm 5\%$ of the recorded value, and that of the fuel mass fraction is expected to be $\pm 1\%$ of the recorded value. The second set of experiments is carried out with $a_2 = 550$ s⁻¹. Here, the temperature of the oxidizer stream $T_{2,i}$ is recorded as a function of $Y_{F,1}$. The results are shown later.

III. Results

A. Extinction of Flames

The mass fraction of the fuel in the fuel stream as a function of the strain rate at extinction is shown in Figs. 2–4 for jet fuels and surrogates. In these figures, the symbols represent experimental data and the lines are best fits to the experimental data. Figure 2 shows that the extinction characteristics of different batches of JP-8 and different batches of Jet-A are similar. FT JP-8 is harder to extinguish in comparison with JP-8 and Jet-A. Figure 3 compares experimental extinction data for potential surrogates of JP-8 with those for JP-8. The extinction characteristics of the surrogates are placed in three groups: group 1 best, group 2 good, and group 3 significant differences. The surrogates placed in these groups are 1) group 1: Drexel surrogate 2, Utah surrogate, surrogate H, and surrogate J;

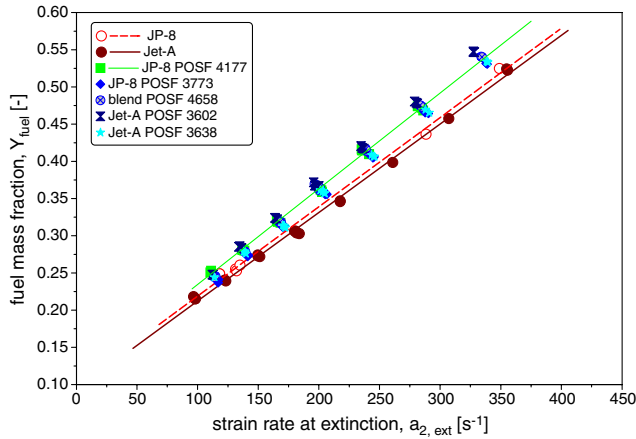


Fig. 2 Mass fraction of fuel as function of strain rate at extinction. Symbols represent experimental data, and lines are best fits to experimental data. The figure compares extinction characteristics of various batches of JP-8, Jet-A, and FT JP-8.

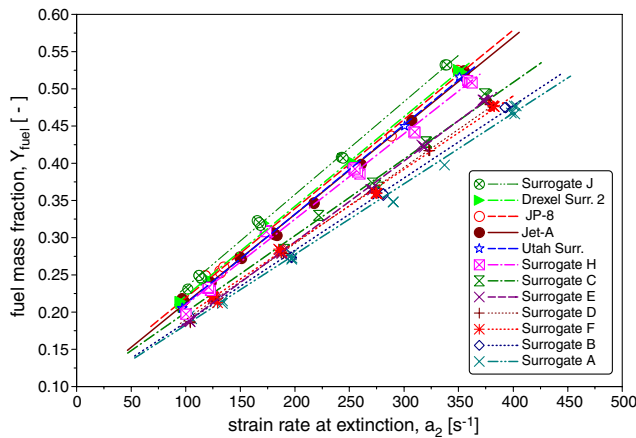


Fig. 3 Mass fraction of fuel as function of strain rate at extinction. Symbols represent experimental data, and lines are best fits to experimental data. The figure compares extinction characteristics of various surrogates of JP-8.

2) group 2: surrogate C, and surrogate E; and 3) group 3: surrogate D, surrogate F, surrogate B, and surrogate A.

Figure 4 shows that the extinction characteristics of surrogate G agree well with those for FT JP-8.

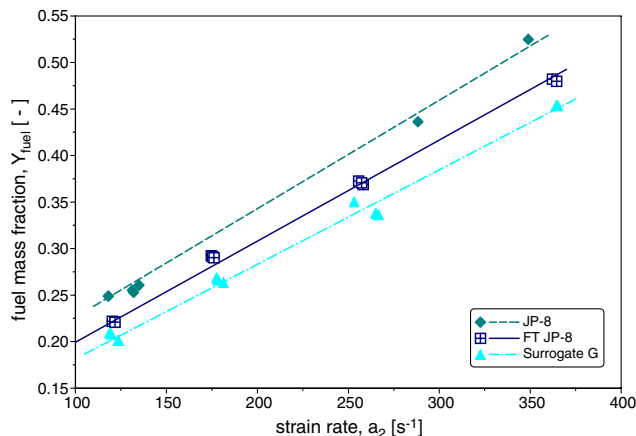


Fig. 4 Mass fraction of fuel as function of strain rate at extinction. Symbols represent experimental data, and lines are best fits to experimental data. The figure compares extinction characteristics of a surrogate and FT JP-8.

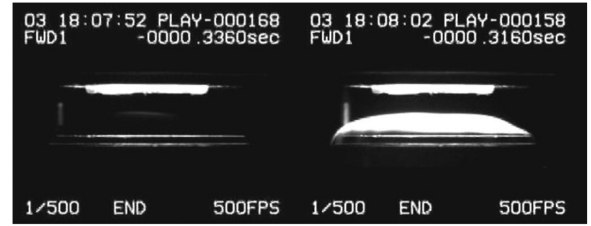


Fig. 5 High-speed photograph of onset of autoignition. The fuel is JP-8 with $a_2 = 427 \text{ s}^{-1}$, $Y_{F,1} = 0.4$, $T_1 = 483 \text{ K}$, $Y_{O_2,2} = 0.23$, and $T_2 = 1225 \text{ K}$.

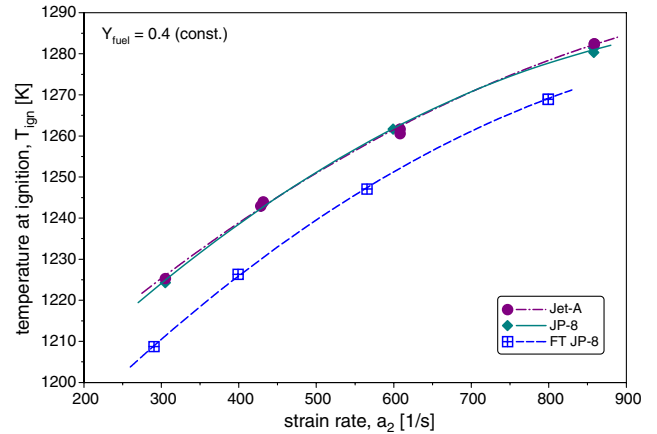


Fig. 6 Temperature of oxidizer stream at autoignition as function of strain rate at fixed values of $Y_{F,1} = 0.4$. Symbols are experimental data. Lines are best fit. The figure compares autoignition characteristics of JP-8, Jet-A, and FT JP-8.

B. Autoignition of Flames

Figure 5 shows photographs of the transient autoignition process recorded by a high-speed camera at 500 frames per second. The fuel is JP-8 with $a_2 = 427 \text{ s}^{-1}$, $Y_{F,1} = 0.4$, $T_1 = 473 \text{ K}$, $Y_{O_2,2} = 0.233$, and $T_2 = 1225 \text{ K}$. The image on the left shows a faint illumination around the axis of symmetry. This is onset of autoignition. The image on the right shows a steady flame. This photograph shows that autoignition takes place around the axis of symmetry.

Figures 6–13 show critical conditions of autoignition. Figures 6, 7, 9, and 11 show the temperature of the oxidizer stream at autoignition as a function of the strain rate for fixed values of $Y_{F,1} = 0.4$. Figures 8, 10, 12, and 13, show the temperature of the oxidizer stream

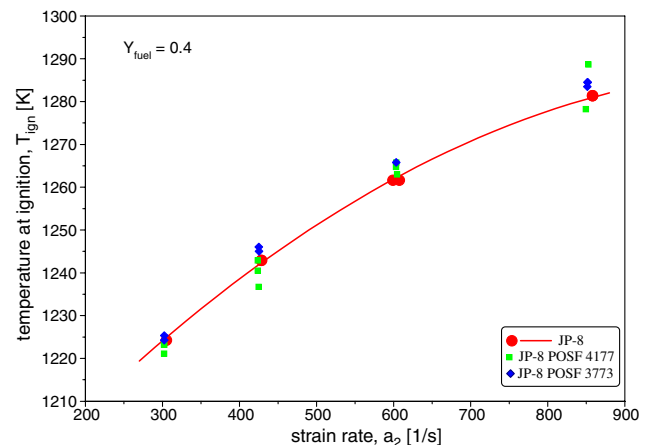


Fig. 7 Temperature of oxidizer stream at autoignition as function of strain rate at fixed values of $Y_{F,1} = 0.4$. Symbols are experimental data. Lines are best fit. The figure compares autoignition characteristics of various batches of JP-8.

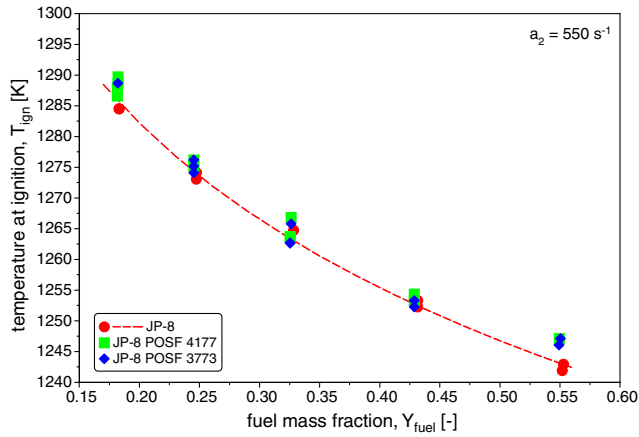


Fig. 8 Temperature of oxidizer stream at autoignition as function of mass fraction of fuel in fuel stream $Y_{F,1}$ at a fixed value of strain rate $a_2 = 550 \text{ s}^{-1}$. Symbols are experimental data. Lines are best fit. The figure compares autoignition characteristics of various batches of JP-8.

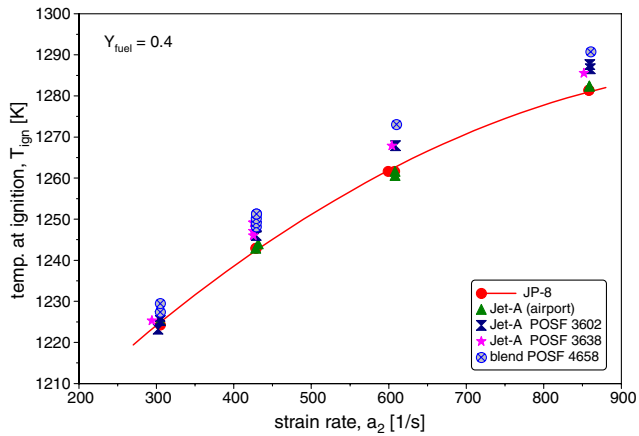


Fig. 9 Temperature of oxidizer stream at autoignition as function of strain rate at fixed values of $Y_{F,1} = 0.4$. Symbols are experimental data. Lines are best fit. The figure compares autoignition characteristics of various batches of Jet-A.

at autoignition as a function of the mass fraction of fuel in the fuel stream $Y_{F,1}$ for fixed values of the strain rate $a_2 = 550 \text{ s}^{-1}$. In these figures, the symbols represent experimental data and the lines are best fits to the experimental data.

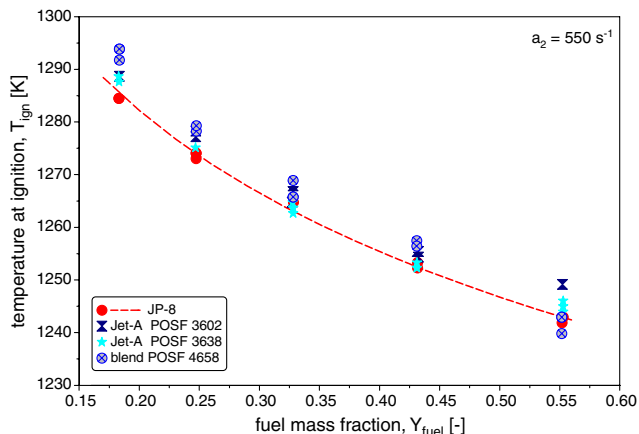


Fig. 10 Temperature of oxidizer stream at autoignition as function of mass fraction of fuel in fuel stream $Y_{F,1}$ at a fixed value of strain rate $a_2 = 550 \text{ s}^{-1}$. Symbols are experimental data. Lines are best fit. The figure compares autoignition characteristics of various batches of Jet-A.

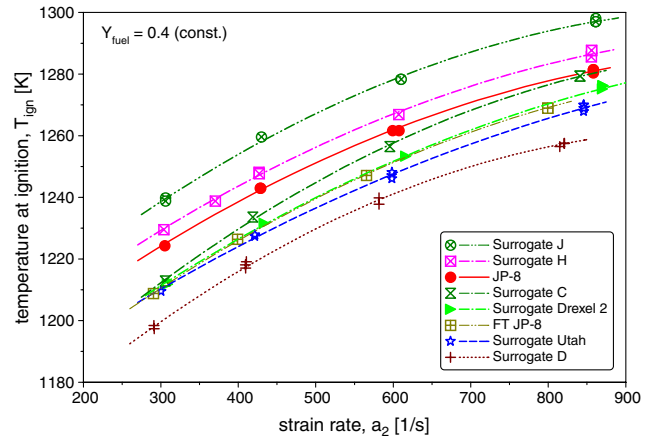


Fig. 11 Temperature of oxidizer stream at autoignition as function of strain rate at fixed values of $Y_{F,1} = 0.4$. Symbols are measurements. Lines are best fit. The figure compares autoignition characteristics of various surrogates of JP-8.

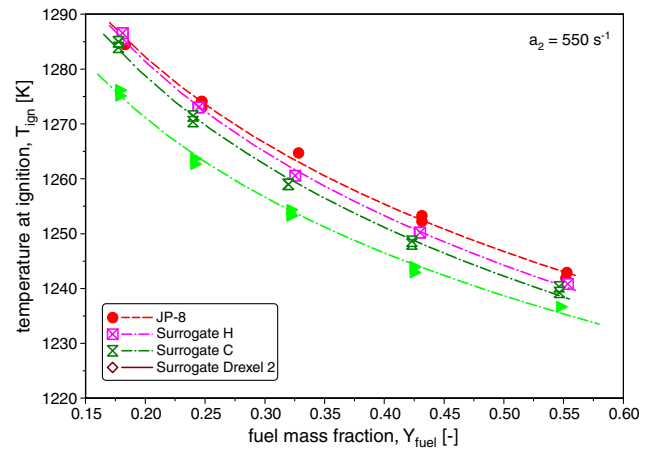


Fig. 12 Temperature of oxidizer stream at autoignition as function of mass fraction of fuel in fuel stream $Y_{F,1}$ at a fixed value of strain rate $a_2 = 550 \text{ s}^{-1}$. Symbols are measurements. Lines are best fit. The figure compares autoignition characteristics of various surrogates of JP-8.

Figure 6 compares the critical conditions of autoignition of JP-8, Jet-A, and FT JP-8. It shows that the autoignition characteristics of JP-8 and Jet-A are similar, while FT JP-8 is easier to ignite. Figures 7 and 8 show that the autoignition characteristics of different

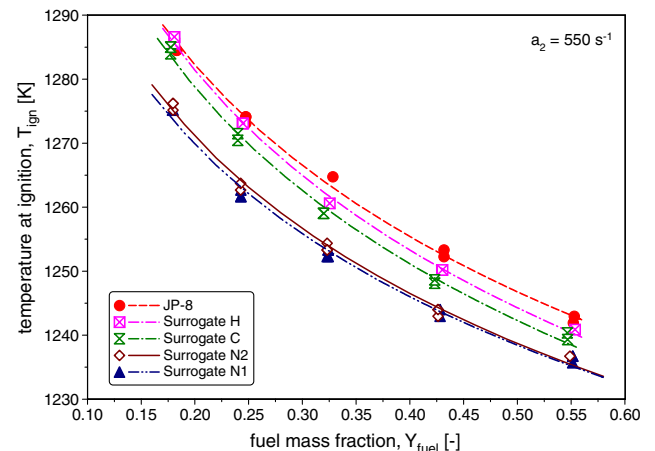


Fig. 13 Temperature of oxidizer stream at autoignition as a function of mass fraction of fuel in fuel stream $Y_{F,1}$ at a fixed value of strain rate $a_2 = 550 \text{ s}^{-1}$. Symbols are measurements. Lines are best fit. The figure compares autoignition characteristics of various surrogates of JP-8.

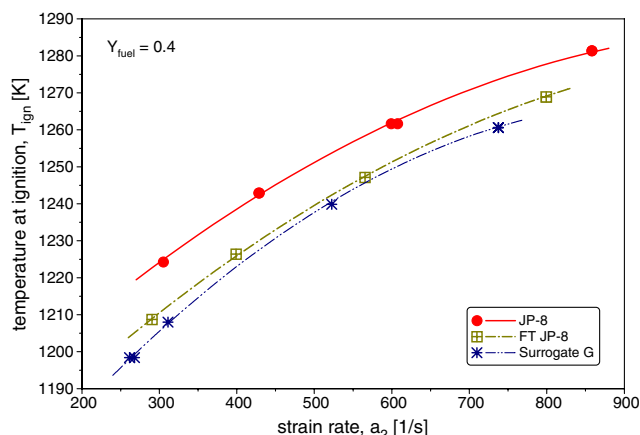


Fig. 14 Temperature of oxidizer stream at autoignition as function of strain rate at fixed values of $Y_{F,1} = 0.4$. Symbols are measurements. Lines are best fit. The figure compares autoignition characteristics of a surrogate of FT JP-8.

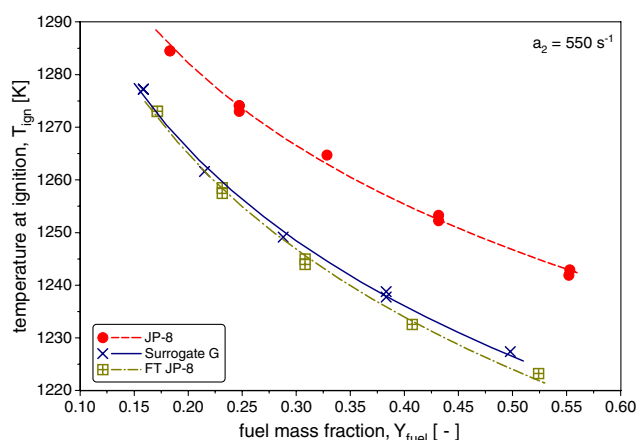


Fig. 15 Temperature of oxidizer stream at autoignition as function of mass fraction of fuel in fuel stream $Y_{F,1}$ at a fixed value of strain rate $a_2 = 550 \text{ s}^{-1}$. Symbols are measurements. Lines are best fit. The figure compares autoignition characteristics of a surrogate of FT JP-8.

batches of JP-8 are the same. Similar results for Jet-A are shown by Figs. 9 and 10.

Figures 11–13 compare experimental autoignition data for potential surrogates of JP-8 with those for JP-8. The autoignition characteristics of the surrogates are placed in three groups: group 1 best, group 2 good, and group 3 significant differences. The surrogates placed in these groups are 1) group 1: surrogate H, and surrogate C; 2) group 2: Drexel surrogate 2, surrogate J, and Utah surrogate; and 3) group 3: surrogate D, surrogate NI, and surrogate N2.

Figures 14 and 15 show that the autoignition characteristics of surrogate G agree well with those for FT JP-8.

IV. Conclusions

The surrogates of JP-8 are ranked employing the following criteria listed in the order of importance: 1) how well they reproduce critical conditions of autoignition, 2) how close the hydrogen-to-carbon ratio is to that of JP-8, 3) simplicity (availability of chemical-kinetic mechanisms), and 4) how well they reproduce critical conditions of extinction. Using this criteria, the surrogates are listed in the following order: 1) surrogate H; 2) surrogate C; 3) Drexel surrogate 2 and surrogate J.

Surrogate H has a H/C ratio of 1.99. Its autoignition characteristics agree best with JP-8 when compared with all surrogates tested here. Its extinction characteristics agree well with JP-8. Surrogate H has

only two components. The chemical-kinetic mechanism for *n*-decane is well known [36]. There is a need to compare the low- and intermediate-temperature chemistries of this surrogate with those for JP-8.

Surrogate C has a H/C ratio of 1.92. This is very close to that of JP-8. The components in the surrogate match the classes of fuel in JP-8. Its autoignition characteristics agree very well with JP-8. Its extinction characteristics agree with JP-8, although some differences are observed. It has only three components. Chemical-kinetic mechanisms for the components of this surrogate are available [7]. In a previous study, critical conditions of extinction and autoignition have been predicted for this surrogate using a detailed chemical-kinetic mechanism, and the results were found to agree with experimental data [7]. There is a need to compare the low- and intermediate-temperature chemistries of this surrogate with those for JP-8.

The Drexel surrogate 2 has a H/C ratio of 1.87. Its autoignition characteristics agree well with JP-8. Its extinction characteristics agree best with JP-8 in comparison with all surrogates tested. The chemical-kinetic mechanisms for the components in this surrogate are in the early stages of development. The low- and intermediate-temperature chemistries of this surrogate agree well with those for JP-8.

Surrogate J has a H/C ratio of 1.97. Its autoignition and extinction characteristics agree well with JP-8. It has only two components. Many investigators are developing chemical-kinetic mechanisms for the components. There is a need to compare the low- and intermediate-temperature chemistries of this surrogate with those for JP-8.

The composition of surrogate H is similar to the composition of the Aachen surrogate tested by Honnet et al. [9]. Overall, surrogate H and surrogate C appear to best reproduce the combustion characteristics of JP-8. Surrogate G reproduces the combustion characteristics of FT JP-8.

Appendix: Analysis of Jet Fuel

Experiments were carried out to confirm that no decomposition of Jet-A and JP-8 takes place in the vaporizer and/or in the fuel lines of the counterflow burner, where its vapors are carried in hot nitrogen toward the burner. Figure A1 shows a schematic illustration of the configuration employed in the experiments. A heated line was attached to the exit of the fuel duct. This line carried the mixtures of fuel vapors and nitrogen to a condenser and an aerosol filter. The condensed fuel vapors from the condenser and the aerosol filter were analyzed in a GC/MS system. The vapors that remained in the nitrogen stream after the aerosol filter were analyzed in a gas chromatograph (GC).

The temperatures in the flow lines between the vaporizer and the fuel duct were measured using thermocouples at various locations. The conditions for this experiment were as follows. Jet-A POSF 3638 was tested. The temperature of the vaporizer was 513 K. Different temperatures were recorded on the flow lines between the vaporizer and the fuel duct with a local maximum of 563 K. The temperature at the exit of the fuel duct was $T_1 = 493 \text{ K}$. In the fuel stream, the mass fraction of fuel was $Y_{F,1} = 0.228$ and the velocity $V_1 = 0.375 \text{ m/s}$ with an approximately equal curtain coflow velocity. This corresponds to a strain rate of $a_2 = 128 \text{ s}^{-1}$ when the momenta of the counterflowing streams are balanced. Portions of Jet-A were collected in the condenser and the aerosol filter, and a liquid sample was created by mixing the two portions together in approximately the same ratio as they were collected in the two units. A reference sample was taken from the original Jet-A. The two samples were analyzed in the GC/MS system. Figure A2 shows the comparison of the two samples. Here, the total mass count of the mass-selective detector is plotted versus the time it takes for a component to travel through the GC column and reach the detector. It can be seen from these results that the chromatograms are nearly identical and that there is no major shift from any major fuel groups to others. Most peaks are preserved and have about equal height between the two samples, i.e., within the accuracy of the instrument.

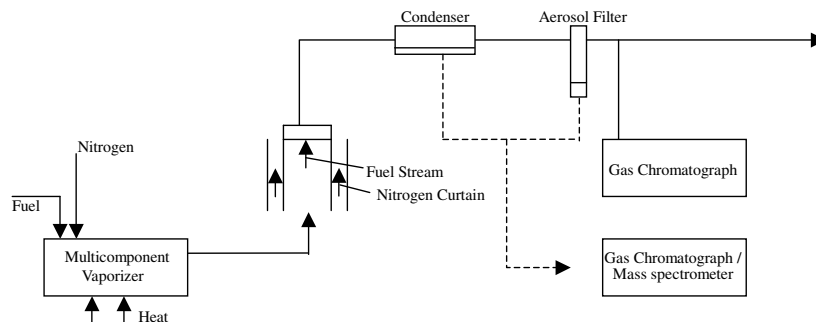


Fig. A1 Schematic illustration of experimental setup employed for measuring composition of fuel vapors at fuel boundary.

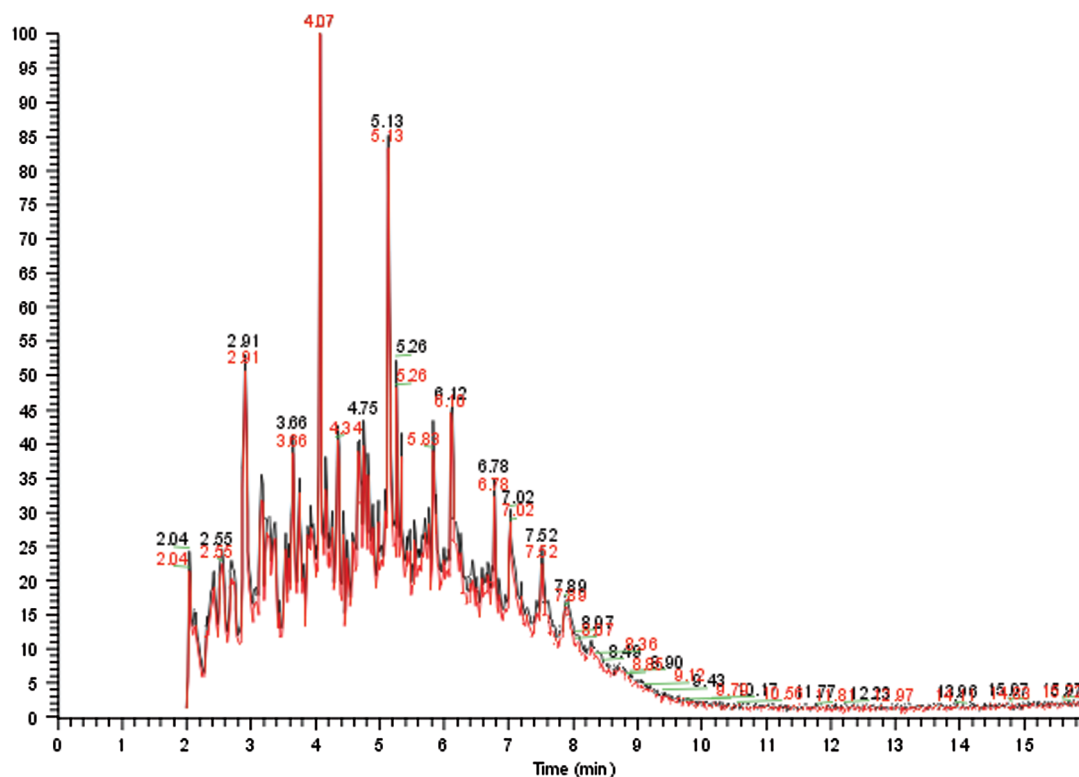


Fig. A2 GC/MS output of components of Jet-A.

A second test was performed to find if there were any smaller hydrocarbon species formed by thermal breakdown of the fuel in the vaporizer. These species would not be detected in the GC/MS system, which is limited to species with a molecular weight of approximately above 100 kg/kmol. Some of these species will not condense in the condenser and aerosol filter, but they could leave the system as vapors. A GC was used to monitor these gases/vapors, as shown in Fig. A1. A GC-column combination of a molecular sieve and a Porapak Q column was used to separate the species, and a flame-ionization detector (FID) was used to detect them. A sampling line was connected from the end of the flow arrangement to the sample loop in the GC. To measure components already present and dissolved in the original Jet-A, a liquid sample (0.002 ml) was injected with a syringe into the instrument's injection port. The chromatograms of both analyses are shown in Fig. A3.

There are four peaks easily identified in the chromatogram of the exit gas (bottom line). When compared with the reference (top line), it is seen that all four components are present in the original fuel. The relative amounts are also consistent, since it is expected that more volatile species (peaks toward the left) are enriched in the exit gas compared with less volatile species (peaks toward the right), since the vaporization and condensation in effect represent a distillation step.

In summary, no new species (that could be products of fuel breakdown) were detected in the analysis of the vapors leaving the experiment. These experiments clearly prove that the jet fuels do not decompose in the fuel lines.

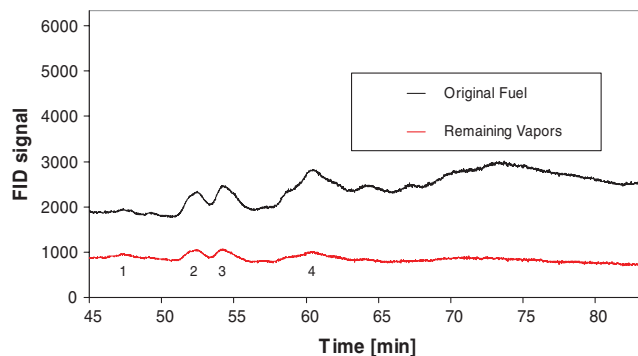


Fig. A3 GC output of components of Jet-A. Top curve represents the original fuel. Bottom curve represents analysis of gaseous products collected after the aerosol filter shown in Fig. A1.

Further tests were carried out to test the differences in composition of different batches of Jet-A and differences between JP-8 and Jet-A. In general, the major peaks were similar.

Acknowledgment

The research at the University of California, San Diego, was supported by the U. S. Army Research Office, grant W911NF-09-1-0108 (program manager, Ralph A. Anthenien, Jr.).

References

- [1] Colket M., Edwards J. T., Williams S., Cernansky N. P., Miller D. L., Egolfopoulos F., Lindstedt P., Seshadri K., Dryer F. L., Law C. K., Friend D. G., Lenhart D. B., Pitsch H., Sarofim A., Smooke M., and Tsang W., "Development of an Experimental Database and Kinetic Models for Surrogate Jet Fuels," 45th AIAA Aerospace Sciences Meeting and Exhibit, Reno, NV, AIAA Paper 2007-770, 2007.
- [2] Agosta, A., Cernansky, N. P., Miller, D. L., Faravelli, T., and Ranzi, E., "Reference Components of Jet Fuels: Kinetic Modeling and Experimental Results," *Experimental Thermal and Fluid Science*, Vol. 28, No. 7, 2004, pp. 701–708.
doi:10.1016/j.expthermflusc.2003.12.006
- [3] Edwards, T., and Maurice, L. Q., "Surrogate Mixtures to Represent Complex Aviation and Rocket Fuels," *Journal of Propulsion and Power*, Vol. 17, No. 2, 2001, pp. 461–466.
doi:10.2514/2.5765
- [4] Edwards, T., "'Real' Kerosene Aviation and Rocket Fuels: Compositions and Surrogates," 2001 Fall Technical Meeting, Eastern States Section of the Combustion Institute, Combustion Inst., Pittsburgh, PA, 2001.
- [5] Violi, A., Yan, S., Eddings, E. G., Sarofim, A. F., Granata, S., Faravelli, T., and Ranzi, E., "Experimental Formulation and Kinetic Model for JP-8 Surrogate Mixtures," *Combustion Science and Technology*, Vol. 174, No. 11, 2002, pp. 399–417.
doi:10.1080/001022002108008
- [6] Maurice, L. Q., "Detailed Chemical Kinetic Models for Aviation Fuels," Ph.D. Thesis, Univ. of London, London, 1996.
- [7] Humer, S., Frassoldati, A., Granata, S., Faravelli, T., Ranzi, E., Seiser, R., and Seshadri, K., "Experimental and Kinetic Modeling Study of Combustion of JP-8, its Surrogates and Reference Components in Laminar Nonpremixed Flows," *Proceedings of the Combustion Institute*, Vol. 31, No. 1, 2007, pp. 393–400.
doi:10.1016/j.proci.2006.08.008
- [8] Schulz, W. D., "Oxidation Products of a Surrogate JP-8 Fuel," *Preprints/Division of Petroleum Chemistry, American Chemical Society*, Vol. 37, No. 37, 1991, pp. 383–392.
- [9] Honnet, S., Seshadri, K., Niemann, U., and Peters, N., "A Surrogate Fuel for Kerosene," *Proceedings of the Combustion Institute*, Vol. 32, No. 1, 2009, pp. 485–492.
doi:10.1016/j.proci.2008.06.218
- [10] Humer, S., Seshadri, K., and Seiser, R., "Combustion of Jet Fuels and its Surrogates in Laminar Nonuniform Flows," 5th U. S. Combustion Meeting, Univ. of California, San Diego Paper E09, San Diego, CA, 2007.
- [11] Holley, A. T., Dong, Y., Andac, M. G., Egolfopoulos, F. N., and Edwards, T., "Ignition and Extinction of Non-Premixed Flames of Single-Component Liquid Hydrocarbons, Jet Fuels, and Their Surrogates," *Proceedings of the Combustion Institute*, Vol. 31, No. 1, 2007, pp. 1205–1214.
doi:10.1016/j.proci.2006.07.208
- [12] Dean, A. J., Penyzkov, O. G., Sevruck, K. L., and Varatharajan, B., "Autoignition of Surrogate Fuels at Elevated Temperatures and Pressure," *Proceedings of the Combustion Institute*, Vol. 31, No. 2, 2007, pp. 2481–2488.
doi:10.1016/j.proci.2006.07.162
- [13] Guéret, C., Cathonnet, M., Boettner, J. C., and Gaillard, F., "Experimental Study and Modeling of Kerosene Oxidation in a Jet-Stirred Flow Reactor," *Twenty-Third Symposium (International) on Combustion*, Combustion Inst., Pittsburgh, PA, 1990, pp. 211–216.
- [14] Dagaut, P., Reuillon, M., Boettner, J. C., and Cathonnet, M., "Kerosene Combustion at Pressures up to 40 atm: Experimental Study and Detailed Chemical Kinetic Modelling," *25th Symposium (International) on Combustion*, Combustion Inst., Pittsburgh, PA, 1994, pp. 919–926.
- [15] Lindstedt, R. P., and Maurice, L. Q., "Detailed Chemical-Kinetic Model for Aviation Fuels," *Journal of Propulsion and Power*, Vol. 16, No. 2, 2000, pp. 187–195.
doi:10.2514/2.5582
- [16] Patterson, P. M., Kyne, A. G., Pourkashanian, M., and Williams, A., "Combustion of Kerosene in Counterflow Diffusion Flames," *Journal of Propulsion and Power*, Vol. 17, No. 2, 2001, pp. 453–460.
doi:10.2514/2.5764
- [17] Montgomery, C. J., Cannon, S. M., Mawid, M. A., and Sekar, B., "Reduced Chemical Kinetic Mechanisms for JP-8 Combustion," 40th AIAA Aerospace Sciences Meeting and Exhibit, AIAA Paper 2002-0036, 2002.
- [18] Montgomery, C. J., Cremer, M. A., Chen, J. Y., Westbrook, C. K., and Maurice, L. Q., "Reduced Chemical Kinetic Mechanisms for Hydrocarbon Fuels," *Journal of Propulsion and Power*, Vol. 18, No. 1, 2002, pp. 192–198.
doi:10.2514/2.5916
- [19] Colket, M. B., and Spadaccini, L. J., "Scramjet Fuels Autoignition Study," *Journal of Propulsion and Power*, Vol. 17, No. 2, 2001, pp. 315–323.
doi:10.2514/2.5744
- [20] Ciezki, H. K., and Adomeit, G., "Shock-Tube Investigation of Self-Ignition of *n*-Heptane-Air Mixtures Under Engine Relevant Conditions," *Combustion and Flame*, Vol. 93, No. 4, 1993, pp. 421–433.
doi:10.1016/0010-2180(93)90142-P
- [21] Pfahl, U., Fieweger, K., and Adomeit, G., "Self-Ignition of Diesel-Relevant Hydrocarbon-Air Mixtures Under Engine Conditions," *Twenty-Sixth Symposium (International) on Combustion*, Combustion Inst., Pittsburgh, PA, 1996, pp. 781–789.
- [22] Minetti, R., Carlier, M., Ribaucour, M., Therssen, E., and Sochet, L. R., "A Rapid Compression Machine Investigation of Oxidation and Auto-Ignition of *n*-Heptane: Measurements and Modeling," *Combustion and Flame*, Vol. 102, No. 3, 1995, pp. 298–309.
doi:10.1016/0010-2180(94)00236-L
- [23] Griffiths, J. F., Halford-Maw, P. A., and Hand Rose, D. J., "Fundamental Features of Hydrocarbon Autoignition in a Rapid Compression Machine," *Combustion and Flame*, Vol. 95, No. 3, 1993, pp. 291–306.
doi:10.1016/0010-2180(93)90133-N
- [24] Cox, A., Griffiths, J. F., Mohamed, C., Curran, H. J., Pitz, W. J., and Westbrook, C. K., "Extents of Alkane Combustion During Rapid Compression Leading to Single- and Two-Stage Ignition," *Twenty-Sixth Symposium (International) on Combustion*, Combustion Inst., Pittsburgh, PA, 1996, pp. 2685–2692.
- [25] Griffiths, J. F., Halford-Maw, P. A., and Mohamed, C., "Spontaneous Ignition Delays as a Diagnostic of the Propensity of Alkanes to Cause Engine Knock," *Combustion and Flame*, Vol. 111, No. 4, 1997, pp. 327–337.
doi:10.1016/S0010-2180(97)00004-7
- [26] Lignola, P. G., Di Maio, F. P., Marzocchella, A., Mercogliana, R., and Reverchon, E., "JSFR Combustion Processes of *n*-Heptane and Isooctane," *Twenty-Second Symposium (International) on Combustion*, Combustion Inst., Pittsburgh, PA 1988, pp. 1625–1633.
- [27] Bakali, A. E., Unkloff, M. B., Dagaut, P., Frank, P., and Cathonnet, M., "Detailed Kinetic Reaction Mechanism for Cyclohexane Oxidation at Pressure up to Ten Atmospheres," *Proceedings of the Combustion Institute*, Vol. 28, No. 2, 2000, pp. 1631–1638.
doi:10.1016/S0082-0784(00)80561-5
- [28] Doute, C., Delfau, J. L., Akkrich, R., and Vovelle, C., "Experimental Study of the Chemical Structure of Low-Pressure Premixed *n*-Heptane-O₂-Ar Flames," *Combustion Science and Technology*, Vol. 124, No. 1, 1997, pp. 249–276.
doi:10.1080/00102209708935647
- [29] Seiser, R., Truett, L., Trees, D., and Seshadri, K., "Structure and Extinction of Non-Premixed *n*-Heptane Flames," *27th Symposium (International) on Combustion*, Combustion Inst., Pittsburgh, PA, 1998, pp. 649–657.
- [30] Seiser, R., Seshadri, K., Piskernik, E., and Linan, A., "Ignition in the Viscous Layer Between Counterflowing Streams: Asymptotic Theory with Comparison to Experiments," *Combustion and Flame*, Vol. 122, No. 3, 2000, pp. 339–349.
doi:10.1016/S0010-2180(00)00139-5
- [31] Seiser, R., Pitsch, H., Seshadri, K., Pitz, W. J., and Curran, H. J., "Extinction and Autoignition of *n*-Heptane in Counterflow Configuration," *Proceedings of the Combustion Institute*, Vol. 28, No. 2, 2000, pp. 2029–2037.
doi:10.1016/S0082-0784(00)80610-4
- [32] Blouch, J. D., and Law, C. K., "Non-Premixed Ignition of *n*-Heptane and Iso-Octane in a Laminar Counterflow," *Proceedings of the Combustion Institute*, Vol. 28, No. 2, 2000, pp. 1679–1686.
doi:10.1016/S0082-0784(00)80567-6
- [33] Davis, S. G., and Law, C. K., "Laminar Flame Speeds and Oxidation Kinetics of Iso-Octane-Air and *n*-Heptane-Air Flames," *27th*

- Symposium (International) on Combustion*, Combustion Inst., Pittsburgh, PA, 1998, pp. 521–527.
- [34] Seshadri, K., and Williams, F. A., “Laminar Flow Between Parallel Plates with Injection of a Reactant at High Reynolds Number,” *International Journal of Heat and Mass Transfer*, Vol. 21, No. 2, 1978, pp. 251–253.
doi:10.1016/0017-9310(78)90230-2
- [35] Bikas, G., “Kinetic Mechanisms for Hydrocarbon Ignition,” Doktors der Ingenieurwis-Senschaften Thesis, Fakultat für Maschinenwesen, Rheinisch Westfälischen Technischen Hochschule Aachen, Aachen, Germany, 2001.
- [36] Bikas, G., and Peters, N., “Kinetic Modelling of *n*-Decane Combustion and Autoignition,” *Combustion and Flame*, Vol. 126, Nos. 1–2, 2001, pp. 1456–1475.
doi:10.1016/S0010-2180(01)00254-1

T. Liewen
Associate Editor